



1 **A Multi-Scale Daily SPEI Dataset for Drought Monitoring at Observation**

2 **Stations over the Mainland China from 1961 to 2018**

3 Qianfeng Wang^{a, c*}, Jingyu Zeng^a, Junyu Qi^b, Xuesong Zhang^{b, c}, Yue Zeng^a, Wei Shui^a,

4 Zhanghua Xu^a, Rongrong Zhang^a, Xiaoping Wu^a

5 a. Fujian Provincial Key Laboratory of Remote Sensing of Soil Erosion and Disaster

6 Protection/College of Environment and Resource, Fuzhou University, Fuzhou,

7 350116, China

8 b. Earth System Science Interdisciplinary Center, University of Maryland, College

9 Park, 5825 University Research Ct, College Park, MD, 20740, USA

10 c. Joint Global Change Research Institute, Pacific Northwest National Laboratory

11 and University of Maryland, College Park, MD 20740, USA

12

13

14

15

16

17

18

19

20

21

*Corresponding author: Qianfeng Wang

E-mail: wangqianfeng@fzu.edu.cn



22 **Highlights:**

- 23 • The SPEI has been widely used to monitor and assess the drought characteristics.
- 24 • A multi-scale daily SPEI dataset was developed across the mainland China from
- 25 1961 to 2018.
- 26 • The daily SPEI dataset can identify the start and end day of the drought event.
- 27 • The daily SPEI dataset developed is free, open and persistent publicly available
- 28 from this study.

29

30

31

32

33

34

35

36

37

38

39

40

41

42

43



44

45 **Abstract:**

46 The monthly Standardized Precipitation Evapotranspiration Index (SPEI) can monitor
47 and assess drought characteristics with one month or longer drought duration. Based
48 on data from 1961 to 2018 at 427 meteorological stations across the mainland China,
49 we developed a daily SPEI dataset to overcome the shortcoming of coarse temporal
50 scale of monthly SPEI. Our dataset not only can identify the start and end dates of
51 drought events, but also can be used to investigate the meteorological, agricultural,
52 hydrological and socioeconomic droughts with different time scales. In the present
53 study, the SPEI data with 3-month scale were taken as a demonstration example to
54 analyze spatial distribution and temporal changes in drought conditions for the
55 mainland China. The SPEI data with 3-month scale showed no obvious intensifying
56 trends in terms of severity, duration, and frequency of drought events from 1961 to
57 2018. Our drought dataset serves as a unique resource with daily resolution to a
58 variety of research communities including meteorology, geography, and natural
59 hazard studies. The daily SPEI dataset developed is free, open and persistent publicly
60 available from this study. The dataset is publicly available via the figshare portal
61 (Wang et al, 2020), with <https://doi.org/10.6084/m9.figshare.12568280>.

62 **Key words:**

63 **SPEI, mainland China, drought, spatial-temporal, scale, meteorological data**

64

65



66 1. Introduction

67 Drought is one of the most destructive natural hazards worldwide. It can lead to
68 adverse effects on the ecological system, industrial production, agricultural **practice**,
69 drinking water availability, hydrological processes and water quality (Bussi and
70 Whitehead, 2020; Lai et al., 2019; Vicente-Serrano et al., 2012; Wang et al., 2014;
71 Wang et al., 2017). Drought has brought about ca. 221 billion dollars loss during 1960
72 to 2016 reported by the International Disaster Database (EM-DAT), and the drought
73 events in South Asia have influenced over 60 million residents from 1998 to 2001
74 (Agrawala et al., 2001). Unfortunately, the drought is expected to increase in
75 frequency and intensity due to the future warming air temperature (Trenberth et al.,
76 2014; Zambrano et al., 2018). The exacerbated drought conditions have promoted
77 some national legislation (such as drought preparedness and plan) to carry out the risk
78 management and adaptive strategy for drought disasters (Garrick et al., 2017).

79 The various drought types result in the difficulty of drought monitoring and
80 assessment. Drought definition is not unique. Some proposed defining drought
81 according to the water deficit (Wilhite and Glantz, 1985), while others defined
82 drought based on the period of abnormal arid conditions (Eslamian et al., 2017). The
83 popular drought can be classified into four types including (1) meteorological, (2)
84 agricultural, (3) hydrological, and (4) socioeconomic droughts (Mishra and Singh,
85 2010). The meteorological drought results from precipitation deficit or evaporation
86 increases (McKee et al., 1993). The meteorological drought can propagate into the
87 agricultural drought with the lower soil moisture availability, and it also can lead to



88 hydrological drought with lower streamflow and socioeconomic drought with lower
89 water availability (Barella-Ortiz and Quintana-Seguí, 2019; Gevaert et al., 2018). In
90 general, drought indices are normally used to monitor and assess the condition or
91 spatial-temporal characteristic of drought.

92 Many drought indices have been developed for the drought monitoring and
93 assessment, such as the Palmer drought severity index (PDSI) (Dai et al., 2004),
94 standardized precipitation index (SPI) (McKee et al., 1993), vegetation water supply
95 index (VWSI) (Carlson et al., 1994), vegetation health index (VHI) (Kogan, 2002),
96 vegetation temperature condition index (VTCI) (Wan et al., 2004), and other drought
97 indices (Men-xin and Hou-quan, 2016; Wang et al., 2015; Wang et al., 2017). PDSI
98 and SPI are the most popular drought studies worldwide (Dai et al., 2004; McKee et
99 al., 1993), however, they have some limitation. PDSI is only suitable to the
100 agricultural drought through characterizing the soil water deficit, and it cannot
101 identify the meteorological, hydrological, and socioeconomic droughts (Feng and Su,
102 2019). In addition, PDSI limits the spatial comparability of drought due to the fact
103 that it is heavily depending on data calibration (Sheffield et al., 2009; Yu et al., 2014).
104 Although the SPI can monitor and assess different drought types by multiple spatial
105 scales at the monthly time step, it only considers the precipitation factor and neglects
106 effects of evaporation stemmed from temperature and other meteorological factors
107 (Wang et al., 2014; Wang et al., 2017; Yang et al., 2018). To solve the above problems,
108 the Standardized Precipitation Evapotranspiration Index (SPEI), which considers the
109 advantage of both PDSI and SPI, was developed to monitor and assess droughts



110 (Vicente-Serrano et al., 2010). It not only accounts for the effect of evaporation on
111 drought, but also have the capability of spatial comparability and characterizing
112 different drought types with multiple time scales (Feng and Su, 2019; Wang et al.,
113 2015). SPEI has been widely used to delineate drought spatial-temporal evolution,
114 drought characteristics, and impacts of drought at the regional and global scales
115 (Mallya et al., 2016; Wang et al., 2014).

116 However, the commonly used SPEI fails to identify droughts with less than
117 one-month duration (Van der Schrier et al., 2011; Vicente-Serrano et al., 2010). With
118 the future climate change, flash droughts have been recently categorized as a type of
119 extreme climate events. Flash droughts occur along with sudden onset, rapid
120 aggravation, and sudden end of drought leading to severe influences (Pendergrass et
121 al., 2020). It is imperative for monitoring the flash droughts with the short-term
122 duration (e.g., several days). To use the sub-month resolution drought index, we have
123 developed the daily SPEI for the first time, and our daily SPEI has been used to assess
124 the drought and its impacts in previous studies (Wang et al., 2015; Wang et al., 2017).
125 The new SPEI can not only identify the drought with one-month and more than
126 one-month duration, but also monitor the drought with several days duration. In
127 addition, our new daily SPEI has filled the gap in the capability to monitor the onset
128 and duration of droughts. Our daily SPEI has similar principles with the commonly
129 used month SPEI in terms of time accumulation effects (Vicente-Serrano et al., 2010;
130 Wang et al., 2015; Yu et al., 2014). The daily SPEI data with different time scales can
131 also meet the requirement of monitoring and assessing of different drought types



132 (meteorological drought, agricultural drought and hydrological drought) at multi-time
133 scales (Wang et al., 2014).

134 The aim of this study, therefore, is to produce a long record (1961-2018) daily
135 drought index dataset for the whole mainland China. Specifically, we used the new
136 daily SPEI algorithm to produce the multi-time scale drought dataset at a daily time
137 resolution. Meteorological data with 427 stations including multi-factor (daily
138 precipitation, daily average air temperature, daily minimum air temperature, daily
139 maximum air temperature and sunshine) are used. The developed drought dataset at
140 the national scale has the potential to be **sued** to monitor and assess droughts and their
141 impacts for the different sectors.

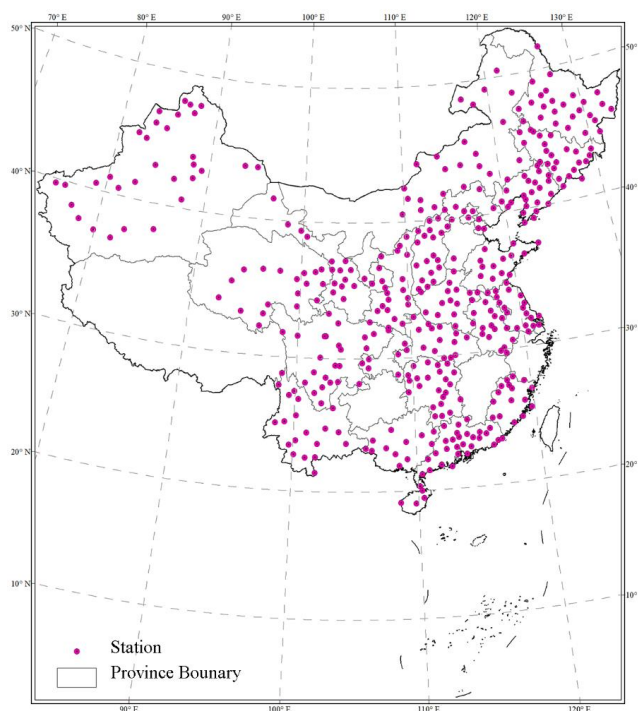
142 **2. Data Sources and Methods**

143 **2.1 Data Sources**

144 Daily meteorological data from 1960 to 2018 were collected from the National
145 Meteorological Science Data Sharing Service Platform (<http://data.cma.cn/>). The data,
146 which have gone through quality controlling, have been used in many studies on
147 drought (Li et al., 2019; Wang et al., 2019). In total, there are 839 stations with public
148 data. To ensure continuous and complete data records, we selected 427 stations data
149 by removing stations with missing data exceeding 30 days. Meteorological variables
150 include the minimum and maximum air temperature (°C), precipitation (mm) and
151 sunshine duration (h). The sunshine duration was converted to solar radiation based
152 on the Ångström function (Chen et al., 2010; Wang et al., 2015). The station location



153 is shown in Figure 1.



154

155 **Figure 1.** The location of meteorological stations across the mainland China.

156 **2.2 Daily SPEI Calculation**

157 The daily SPEI can be calculated by the difference between daily precipitation
158 and daily potential evapotranspiration. Because air temperature and solar radiation
159 explained at least 80% of evapotranspiration variability (Martí et al., 2015; Priestley
160 and Taylor, 1972), the Hargreaves model based on temperature and solar radiation can
161 be used to estimate the daily potential evapotranspiration (Hargreaves and Samani,
162 1982; Mendicino and Senatore, 2013; Wang et al., 2015). The daily potential
163 evapotranspiration can be obtained by the following formula:



$$164 \quad PET = 0.0023 * (T_{mean} + 17.8) * \sqrt{(T_{max} - T_{min})} * R_a \quad (1)$$

165 where, T_{mean} is the daily average air temperature ($^{\circ}\text{C}$); T_{max} and T_{min} are the daily
166 maximum and minimum air temperatures ($^{\circ}\text{C}$), respectively; and R_a is the daily net
167 radiation on the land surface ($\text{MJ m}^{-2} \text{d}^{-1}$).

168 SPEI calculation depends on the accumulating deficit or surplus (D_i) of water
169 balance at different time scales. D_i can be determined based on precipitations (P) and
170 PET for a given day i :

$$171 \quad D_i = P_i - PET_i \quad (2)$$

172 The obtained D_i values are summed at different time scales, following the same
173 procedure as that for the commonly used SPEI. The $D_{i,j}^k$ in a given day j and year
174 i depends on the chosen time scale k (days). For example, the accumulated difference
175 for 1 day in a particular year i with a 30-day (or other time scales) time scale is
176 calculated using:

$$177 \quad X_{i,j}^k = \sum_{l=31-k+j}^{30} D_{i-1,l} + \sum_{l=1}^j D_{i,l}, \quad \text{if } j < k \text{ and} \quad (3)$$
$$X_{i,j}^k = \sum_{l=j-k+1}^j D_{i,l}, \quad \text{if } j \geq k$$

178 We also need to normalize the water balance into a probability distribution to get
179 the SPEI index series. The best distribution for SPEI calculation is the generalized
180 extreme value (GEV) distribution (Stagge et al., 2015), which can overcome the
181 limitation of original SPEI through generalized logistic distribution for short
182 accumulation (1–2 months) periods (Stagge et al., 2015; Vicente-Serrano et al., 2010).
183 Therefore, we adopted the GEV distribution to standardize the D series into SPEI data
184 series (Monish and Rehana, 2020). The GEV probability density function is:



$$f(x) = \begin{cases} \left(\frac{1}{\sigma}\right) \left[(1 + \xi z(x))^{-1/\xi} \right]^{\xi+1} e^{-[(1+\xi z(x))^{-1/\xi}]}, & \xi \neq 0, 1 + \xi z(x) > 0 \\ \left(\frac{1}{\sigma}\right) e^{-z(x) - e^{-z(x)}}, & \xi = 0, -\infty < x < \infty \end{cases}$$

185
 186 (4)
 187

where,

$$z(x) = \frac{x - \mu}{\sigma} \tag{5}$$

188
 189

190 where, ξ , σ , and μ are the shape, scale, and location parameters respectively.

191 The cumulative distribution function $F(x)$ of GEV can be calculated by the
 192 following equation:
 193

$$F(x) = e^{-t(x)} \tag{6}$$

194
 195

where,

$$t(x) = \begin{cases} \left(1 + \xi \left(\frac{x - \mu}{\sigma} \right) \right)^{-1/\xi}, & \text{if } \xi \neq 0 \\ e^{-(x - \mu)/\sigma}, & \text{if } \xi = 0 \end{cases} \tag{7}$$

197 Thus, the probability distribution function of the D series is given by:

$$F(x) = \left[1 + \left(\frac{\alpha}{x - \gamma} \right)^\beta \right]^{-1} \tag{8}$$

198 With $F(x)$, the SPEI can easily be obtained as the standardized values of $F(x)$.

199 Following the classical approximation of Abramowitz and Stegun (1965):
 200

$$SPEI = W - \frac{C_0 + C_1 W + C_2 W^2}{1 + d_1 W + d_2 W^2 + d_3 W^3} \tag{9}$$

202 where, $W = \sqrt{-2 \ln(P)}$ for $P \leq 0.5$ and P is the probability of exceeding a
 203 determined D value, $P = 1 - F(x)$. If $P > 0.5$, then P is replaced by $1 - P$ and the sign



204 of the resultant SPEI is reversed. The constants are $C_0 = 2.515517$, $C_1 = 0.802853$,
205 $C_2 = 0.010328$, $d_1 = 1.432788$, $d_2 = 0.189269$, and $d_3 = 0.001308$.

206 2.3 Drought Analysis Method

207 The daily SPEI dataset were calculated at multi-time scales (1-month, 3-months,
208 6-months, 9-months and 12-months) using the daily meteorological data from
209 1960-2018 at 427 station locations. The classifications for the SPEI drought classes
210 are presented in Table 1.

211

212 Table 1 Categorization of drought and wet grade according to the SPEI.

Categorization	SPEI values
Extremely Wet	$\text{SPEI} \geq 2$
Severe Wet	$1.5 \leq \text{SPEI} < 2$
Moderate Wet	$1 \leq \text{SPEI} < 1.5$
Mild Wet	$0.5 < \text{SPEI} < 1$
Normal	$-0.5 \leq \text{SPEI} \leq 0.5$
Mild Drought	$-1 < \text{SPEI} < -0.5$
Moderate Drought	$-1.5 < \text{SPEI} \leq -1$
Severe Drought	$-2 < \text{SPEI} \leq -1.5$
Extremely Drought	$\text{SPEI} \leq -2$

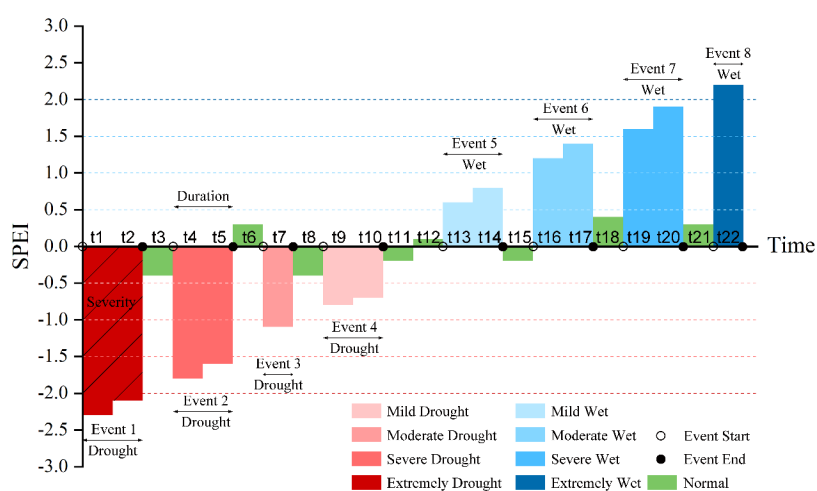
213

214 We used the method described by Yevjevich (1967) **too** define the drought
215 characteristics (severity, duration, and intensity). A drought event can be firstly
216 determined by drought start and end dates, and its duration and severity were then
217 assigned. Thus, we accounted for the continuity of drought propagation. The
218 continuous days with SPEI values less than the threshold (such as -0.5,-1.0,-1.5,-2)
219 are defined as the duration of a drought event \dots The severity is the integral area
220 between absolute value of the SPEI with value < -0.5 and the horizontal axis (SPEI = 0)



221 from the drought start day to the drought end day. The drought frequency is the total
222 number of drought events in a period. The drought event and its characteristics
223 (severity, duration, and intensity) can be demonstrated in Figure 2.

224



225

226 **Figure 2.** Schematic diagram of drought and wet events (the red shaded area
227 denotes the drought events; the blue shaded area denotes the wet events).

228

229 The SPEI data based on 90-day (3-month) time scales can be used to identify soil
230 moisture or agriculture droughts (Wang et al., 2014). Due to its important applications,
231 we selected the SPEI data with the 90-day time scales as the example data for
232 analyzing in the present study. To investigate the spatial-temporal characteristics of
233 the example data, we defined three variables including Annual Total Drought Severity
234 (ATDS), Annual Total Drought Duration (ATDD), and Annual Total Drought
235 Frequency (ATDF). The three variables were obtained by summing the severity,
236 duration, and frequency of all the drought events in each year at 427 stations.

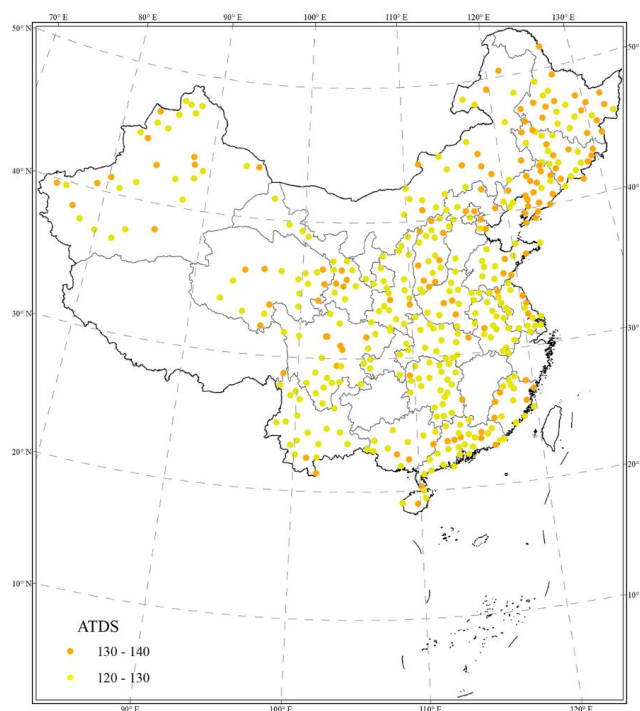


237 We also used the non-parametric Mann–Kendall (MK) test to detect monotonic
238 trends (Kendall, 1948; Mann, 1945), and computed slopes for ATDS, ATDD and ADF
239 using the Sen’s method (Sen, 1968). These statistical methods are commonly used in
240 analyses of water resources, climate, and ecology data. For the MK test, the global
241 trend for the entire series is significant when P-value < 0.05.

242 **3 Analysis Results**

243 **3.1 Spatial Distribution of Drought Characteristics**

244 The ATDS can be used to identify hot spots with severer drought conditions. Figure
245 3 shows the calculated ATDS values across the mainland China. We categorized
246 ATDS values into two main groups with higher ATDS values indicated more severe
247 drought conditions. The distribution of ATDS values shows that, in general,
248 northeastern parts of China had more severe drought conditions than southern parts.
249 However, our results also indicate that the humid climate zone in the south also
250 experienced severe drought conditions, though not as much as for northern parts of
251 China (Figure 3).



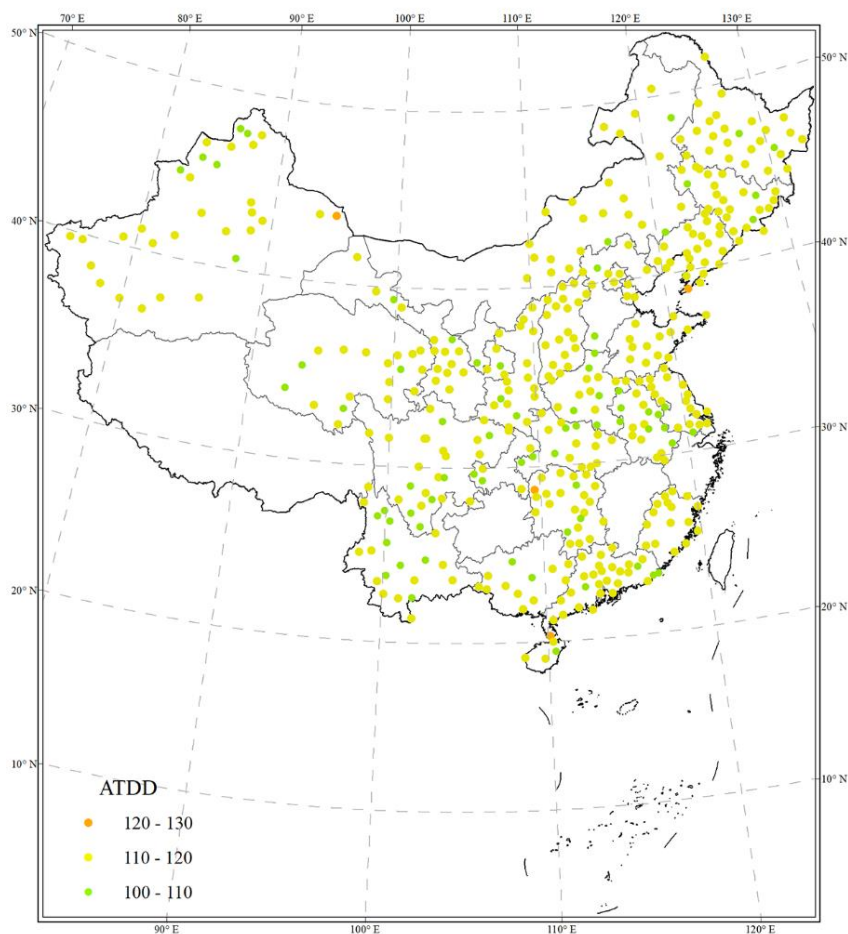
252

253

Figure 3. The spatial distribution of ATDS across the mainland China.

254

255 Figure 4 shows that ATDD values ranged from 100 to 110 days for most stations
256 across the mainland China. This indicates that there was near one-third of a year when
257 most stations were experiencing drought conditions. More stations with ATDD values
258 ranging from 100 to 110 were found compared with stations with ATDD values of
259 120-130 (Fig. 4). For drought years, the duration days of drought events are expected
260 to be ~~were~~ longer. The ATDD had similar spatial distribution characteristics with the
261 ATDS, indicating that droughts also occurred in the humid climate zone.



262

263

Figure 4. The spatial distribution of ATDD across the mainland China.

264

265

Figure 5 shows the spatial distribution of ATDF values across the mainland China.

266

In general, most stations had 4-6 annual drought events. There were fewer stations

267

with 6-8 annual drought events compared with stations with 2-4 annual drought

268

events. We also detected that drought events could be occurring in both arid and

269

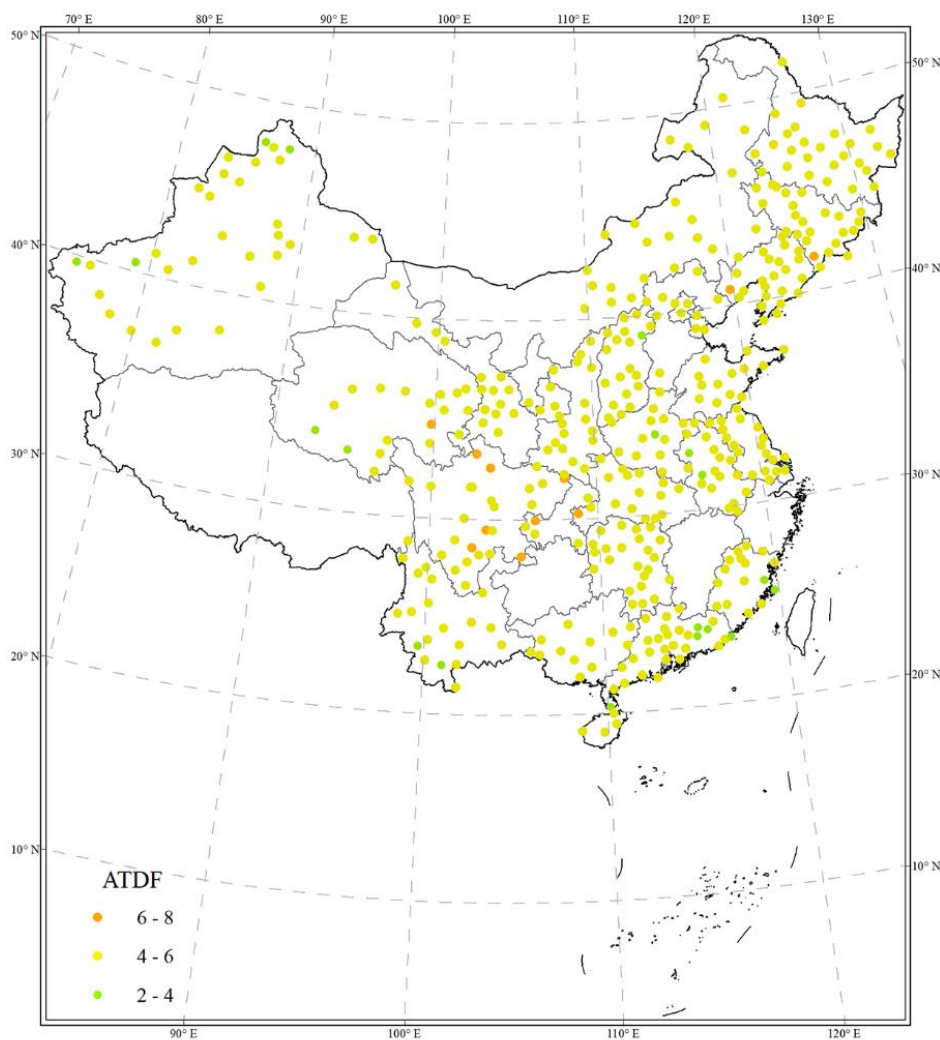
humid regions based on spatial distributions of ATDF values (Figure 5). Since the

270

ATDF indicated only the annual average drought events, we could expect that for the



271 severer drought years the ATDF would have greater values for different stations.



272

273 **Figure 5.** The spatial distribution of ATDF across the mainland China.

274

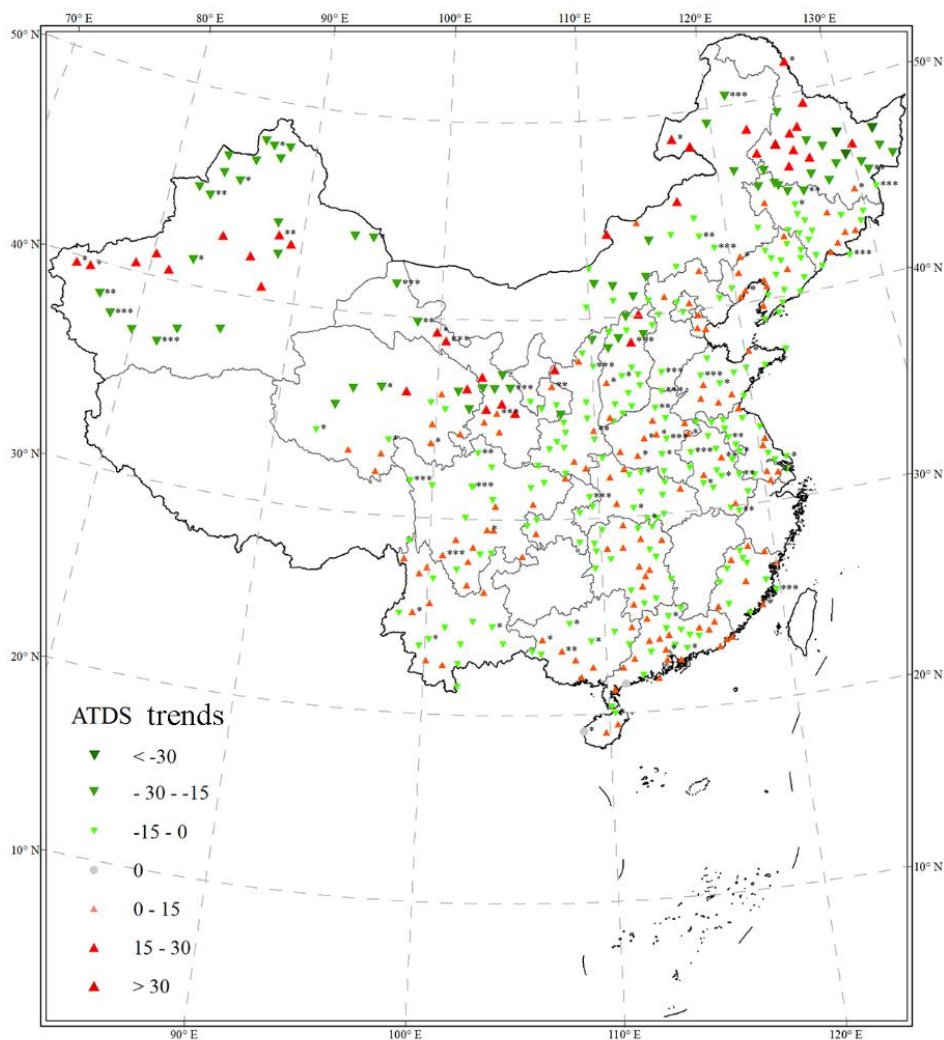
275 3.2 Trends in Drought Characteristics

276 The changing trends of ATDS can be used to detect whether drought severity is

277 weakening or intensifying with time, Figure 6 shows that the spatial distribution of



278 changing trends of ATDS from 1961 to 2018 across the mainland China. In general,
279 there were more stations with weakening trends in drought severity than those with
280 intensifying trends across all stations (Figure 6). It seems that both weakening and
281 intensifying absolute values were largest in the northeast, northwest, and central
282 China compared with other parts. However, after scrutiny, we found that drought
283 severity tended to weaken in the northeast, northwest, and center China with more
284 stations having significant weakening trends by statistical test (P-value<0.05; Figure
285 6). For southern China, most stations had no significant trends in either weakening or
286 intensifying of drought severity (P-value>0.05; Figure 6).



287

288 **Figure 6.** The spatial distribution of the changing trends of ATDS (the red and green
289 triangular indicate increasing and decreasing trends, respectively. “****” denotes
290 P-value < 0.001, “***” denotes P-value < 0.01, and “**” denotes P-value < 0.05).

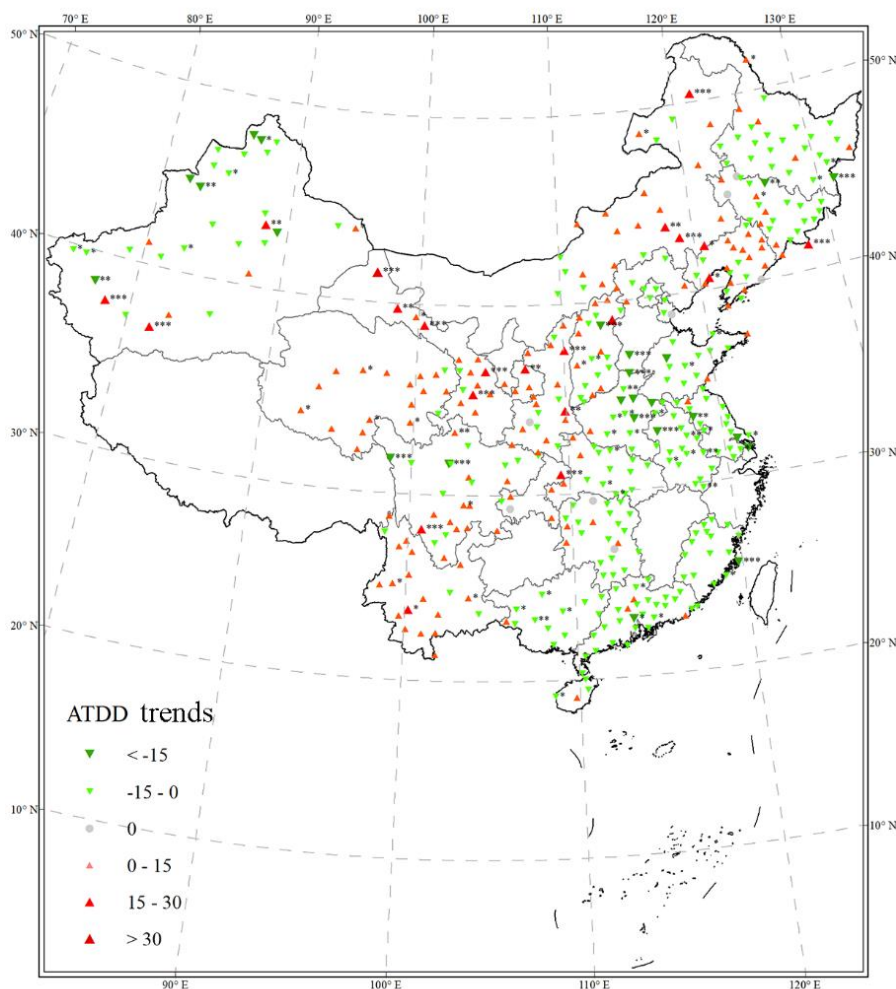
291

292 The changing trends of ATDD can be used to detect whether drought duration is
293 getting shorter or longer. Figure 7 shows the spatial distribution of changing trends for



294 the ATDD across all stations. In general, stations in the southeast demonstrated
295 downward trends with shortening drought duration, while stations in the northwest
296 had upward trends for the ATDD with increasing drought duration (Figure 7). Note
297 that the increasing or decreasing trends for ATDD were significant (P value < 0.05)
298 for stations across the central China indicating that the central China regions were
299 suffering dramatic changes of drought conditions.

300



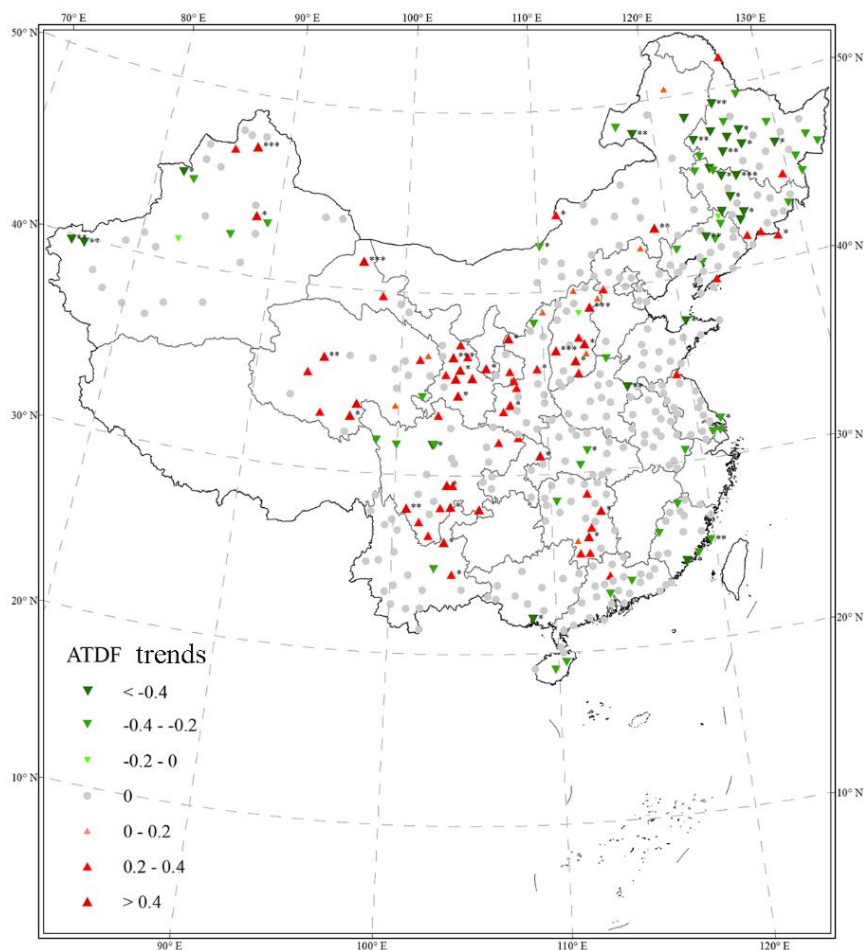
301



302 **Figure 7.** The spatial distribution of the changing trends of ATDD (the red and green
303 triangular indicate increasing and decreasing trends, respectively. “****” denotes
304 P-value < 0.001, “***” denotes P-value < 0.01, and “*” denotes P-value < 0.05).

305

306 The changing trends of ATDF can be used to detect whether the frequency of
307 drought events is increasing or decreasing with time. Figure 8 shows the spatial
308 distribution of changing trends of ATDF across all stations. Most stations
309 demonstrated no significant trend in the frequency of drought events, except for
310 dozens of stations in western China having significant upward trends (P-value < 0.05)
311 with increasing frequency in drought events, and stations in northeastern China
312 demonstrated significant downward trends (P-value < 0.05) with decreasing
313 frequency of drought events.



314

315 **Figure 8.** The spatial distribution of the changing trends of ATDF (the red and green
316 triangular indicate increasing and decreasing trends, respectively. “***” denotes
317 P-value < 0.001, “**” denotes P-value < 0.01, and “*” denotes P-value < 0.05).

318

319



320 4. Discussion

321 The reason for selecting 3-month scale to assess spatial and temporal
322 characteristics of drought conditions across the mainland China is because the SPEI
323 with the 3-month scale can indicate the agricultural drought (or soil moisture) (Van
324 der Schrier et al., 2011; Wang et al., 2014; Wang et al., 2017), and its results are
325 comparable with the PDSI (Dai et al., 2004; Van der Schrier et al., 2011) and other
326 drought indices including Surface Water Supply Index (SWSI) and Moisture
327 Adequacy Index(MAI) (Doesken and Garen, 1991; McGUIRE and Palmer, 1957).
328 The commonly used monthly SPEI have been used to assess drought characteristics
329 and their impacts worldwide from the regional scale to the global scale (Stagge et al.,
330 2015; Vicente-Serrano et al., 2010; Wang et al., 2014). The SPEI with different time
331 scales is relevant for meteorological drought (1-month timescale), agricultural drought
332 (3-6-month timescale), hydrological drought (12-month timescale), and
333 socioeconomic drought (24-month timescale), respectively (Homdee et al., 2016;
334 Potop et al., 2014; Tirivarombo et al., 2018; Vicente-Serrano et al., 2010).

335 Our new SPEI dataset with multi-time scales were developed and compiled using
336 the daily SPEI algorithm in the previous study (Wang et al., 2015). The daily SPEI
337 has been used in drought monitoring and assessment, and was validated by drought
338 monitoring and assessment (Jevšenak, 2019; Jia et al., 2018; Salvador et al., 2019;
339 Wang et al., 2015; Wang et al., 2017). The global SPEI database with monthly
340 temporal resolution and 0.5 degree spatial resolution is available



341 (<https://spei.csic.es/database.html>). The database covers the period between January
342 1901 and December 2018. Although the database can be used effectively for the
343 meteorological, agricultural, hydrological, and socioeconomic droughts, it cannot
344 identify and detect the flash drought with less than one-month duration. In addition,
345 the database can only detect the start month and end month of drought events, and
346 therefore it fails to determine the start and end dates of a drought event, the monthly
347 SPEI (Kassaye et al., 2020; Vicente-Serrano et al., 2010; Wang et al., 2014). Our
348 newly developed daily SPEI can compensate the shortcomings of monthly SPEI in
349 drought monitoring and assessment. In addition, we used the well-received GEV
350 probability distribution for the SPEI calculation for our dataset (Stagge et al., 2015).

351 Although the daily SPEI has better performance in drought monitoring and
352 assessment (Jevšenak, 2019; Wang et al., 2017), the uncertainty of daily SPEI still
353 needs to be evaluated in future works. Our daily SPEI dataset used the simple
354 Hargreaves model based on temperature and solar radiation to estimate daily potential
355 evapotranspiration (Hargreaves and Samani, 1982; Wang et al., 2017). We will further
356 investigate effects of various evapotranspiration models (such as CRAE model,
357 Penman algorithm, Thornthwait algorithm, Makkink algorithm, and Priestley–Taylor
358 algorithm) on the calculation of SPEI (Makkink, 1957; Morton, 1983; Penman, 1948;
359 Priestley and Taylor, 1972; Thornthwaite, 1944). We only chose SPEI based on the
360 3-month timescale as an example to analyze drought characteristics, and the results
361 demonstrated that there was no obvious intensifying trends for drought across the
362 mainland China which is consistent with other studies (Han et al., 2020). Meanwhile,



363 our newly developed daily SPEI will be validated in other regions of the world.

364 Our long-term daily SPEI dataset has contributed significantly to our
365 understanding of drought evolution, especially flash drought. The dataset can be used
366 to monitor and assess different drought types (meteorological drought, agricultural
367 drought, and hydrological drought) through different timescale data. It also can
368 identify the start and end dates for drought. Our daily SPEI dataset not only have the
369 capability of monitoring and assessing droughts, but also can be used to evaluate the
370 impact of droughts on ecological system and natural resources. The dataset is valuable
371 to meteorological research and natural hazards communities for various purposes such
372 as assessment of extreme climate or drought effect evaluation.

373 **5. Data Availability**

374 All daily SPEI dataset including data and their description at 427 observed
375 meteorological stations, the data is also provided as open access via figshare (Wang et
376 al, 2020), available at doi: doi.org/10.6084/m9.figshare.12568280. This depository
377 includes the five files directory of the daily SPEI data with five scales (1 month, 3
378 month, 6 month, 12 month, 24 month) and station information for 427 meteorological
379 stations.

380 **6. Summary**

381 In the present study, we have produced a daily SPEI dataset from 1960 to 2018 at
382 427 meteorological stations across the mainland China. Our open-access dataset is an



383 important contribution to drought assessment, and it can overcome the disadvantages
384 of the commonly used monthly SPEI database. Our daily dataset can help monitor and
385 assess the spatial and temporal characteristics of droughts. It can be used to assess the
386 impacts of droughts on ecological system, hydrological processes, and other natural
387 resources. Our multi-time scale daily SPEI dataset can be widely used in studies on
388 meteorological drought (1-month timescale), agricultural drought (3-6-month
389 timescale), hydrological drought (12-month timescale), and socioeconomic drought
390 (24-month timescale). The dataset will reduce the time spent on research and avoid
391 the duplication of efforts, which will be highly attractive to meteorological,
392 geographical, natural hazard researchers and searchers from other areas.

393

394 **Author contributions.** QFW led the study, developed the method, and wrote the
395 manuscript with input from all the authors. JYQ and XSZ discussed the results and
396 revised the manuscript. All the authors contributed to the final manuscript. QFW, JYZ,
397 RRZ, XPW, and XZZ collected and analysed data over time, providing statistics and
398 material (graphs and tables) for the paper.

399

400 **Competing interests.** The authors declare that they have no conflict of interest.

401 **Acknowledgements.** This research received financial support from the National
402 Natural Science Foundation of China (41601562), the Strategic Priority Research
403 Program of the Chinese Academy of Sciences (XDA13020506) and China
404 Scholarship Council. The authors sincerely thank James Howard Stagge for his help



405 on the codes and calculation of SPEI. Special thanks go to the meteorological data
406 provider from China Meteorological Administration (<http://cdc.cma.gov.cn/>).

407

408 **References:**

409 Agrawala, S., Barlow, M., Cullen, H., and Lyon, B.: The drought and humanitarian
410 crisis in Central and Southwest Asia: a climate perspective, IRI special report N.
411 01-11, International Research Institute for Climate Prediction, Palisades, 24, 2001.

412 Barella-Ortiz, A. and Quintana-Seguí, P.: Evaluation of drought representation and
413 propagation in regional climate model simulations across Spain, *Hydrology and Earth
414 System Sciences*, 23, 5111-5131, 2019.

415 Bussi, G. and Whitehead, P. G.: Impacts of droughts on low flows and water quality
416 near power stations, *Hydrological Sciences Journal*, 65, 898-913, 2020.

417 Carlson, T. N., Gillies, R. R., and Perry, E. M.: A method to make use of thermal
418 infrared temperature and NDVI measurements to infer surface soil water content and
419 fractional vegetation cover, *Remote sensing reviews*, 9, 161-173, 1994.

420 Chen, C., Wang, E., and Yu, Q.: Modelling the effects of climate variability and water
421 management on crop water productivity and water balance in the North China Plain,
422 *Agricultural Water Management*, 97, 1175-1184, 2010.

423 Dai, A., Trenberth, K. E., and Qian, T.: A global dataset of Palmer Drought Severity
424 Index for 1870–2002: Relationship with soil moisture and effects of surface warming,
425 *Journal of Hydrometeorology*, 5, 1117-1130, 2004.

426 Doesken, N. and Garen, D.: Drought monitoring in the Western United States using a